An Energy Band-Pass Filter Using Superlattice Structures

Hsin-Han Tung and Chien-Ping Lee, *Senior Member, IEEE*

Abstract— **A novel quantum mechanical energy band-pass filter (EBPF) using semiconductor superlattices is proposed. Such structures with a Gaussian superlattice potential profile allow the incident electrons to be nearly totally transmitted when the impinging electron energy is in the passband. On the other hand, a complete reflection occurs when the impinging energy is in the stopband. By adjusting the parameters of the potential profile and the superlattice, the desired passband and stopband of such filter can be obtained. Time evolution of an electron wave packet moving through such a structure is calculated by numerically solving the time-dependent Schrödinger equation. The numerical simulation clearly demonstrates the characteristics of total transmission and total reflection. The generalized concept of matched quantum-mechanical wave impedance (QMWI) analogous to that used in the transmission line theory is presented to explain the occurrence of total transmission of the proposed structures.**

I. Introduction

SUPERLATTICE structures have been of considerable interest for many years as means of manipulating electron dispersion in semiconductors [1], [2]. These structures can be created by stacking alternately ultra-thin layers of semiconductor films. Recent developments in epitaxial growth technology have made it possible to control the structure, composition, and doping profile of these artificially structured semiconductors to nearly arbitrary precision. Thus, one can design structures with energy band gap characteristics and more generally band structures exhibiting the desired transport and optical properties for specific applications. Many useful devices such as optical modulators [3], waveguides [4], and infrared photodetectors [5] have been fabricated using these new structures. Investigation of electron propagation in such layered media is of particular interest because the transport property is governed by the minibands formed in the superlattices. Multiple quantum barriers that enhance carrier blocking [6] and resonant tunneling structures that enhance carrier transmission [7] are good examples which demonstrate the current manipulating capability of these structures. However, because of the finite thickness (or number of layers) of the superlattice structures, the minibands for carrier transmission are not really flat "bands." 100% transmission cannot be achieved for all the energies within the bands. Therefore, transporting of carriers with energies in the bands can never be complete. A wavepacket with a finite width or energy impinging upon such a structure will be partially reflected and partially transmitted even its energy lies within a miniband.

Nakagawa *et al.* [8] have considered the problem of electron reflection at the semiconductor/superlattice interface and proposed to use a transition region at the interface to minimize the reflection. The transition region is a linearly graded superlattice which consists of layers with linearly graded potential height. By adding such an antireflection layer, good transmission from the bulk semiconductor to the superlattice was obtained. In this paper, we proposed a new superlattice structure which has the transmission characteristics and reflection characteristics like a perfect "energy" bandpass filter (EBPF). 100% transmission and 100% reflection can be obtained when the electron energy lies within the respective bands. The bands are flat and their positions and the bandwidths are adjustable. Details of the superlattice structures and their transmission characteristics are presented in Section II. The transmission probability is calculated using the transfer-matrix method, which is derived from the plane wave type solution [9] with assumed boundary conditions. The wave equation approach is conceptually simple and it naturally provides the first level of theoretical analysis. In Section III, the time evolution of a Gaussian wave packet moving through this superlattice structure is presented to demonstrate the capability of total transmission or total reflection for EBPF's. In Section IV, we use the concept of matched quantum-mechanical wave impedance (QMWI), which is analogous to the transmission theory, to explain the occurrence of total transmission. Our conclusion is given in Section V.

II. Structure of EBPF Superlattices

Fig. 1 shows the conduction-band edge of the investigated superlattices. The structure can be considered as a regular superlattice modulated by a Gaussian function. a and b are the widths of the potential barriers and the wells, respectively, L is the total length of the superlattice, and V_0 is the largest barrier height. The Gaussian function is expressed by $\exp(-x^2/\sigma_s^2)$, where x is the coordinate in the direction normal to the superlattice and $\sigma_s/\sqrt{2}$ is the standard deviation of the Gaussian function. This potential profile can be obtained, for example, by gradually changing the mole fraction in a GaAs–AlGaAs–InGaAs material system. From the basic quantum theory [10], we know that when electrons are moving in a region where the spatial variation

Manuscript received May 30, 1995; revised September 15, 1995. This work is supported by the National Science Council of the Republic of China under contract no. NSC84-2215-E009-039.

H.-H. Tung is with the Department of Electronics Engineering, National Chiao Tung University, Hsin-Chu 300, Taiwan, ROC. He is also with the Department of Electrical Engineering, Lien-Ho College of Technology, Miao-Li 360, Taiwan, ROC.

C.-P. Lee is with the Department of Electronics Engineering, National Chiao Tung University, Hsin-Chu 300, Taiwan, ROC.

Publisher Item Identifier S 0018-9197(96)02041-6.

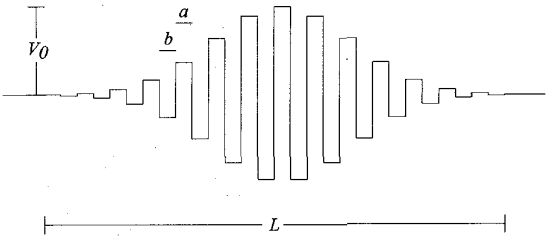

Fig. 1. Schematic diagram of potential profile for an EBPF superlattice structure.

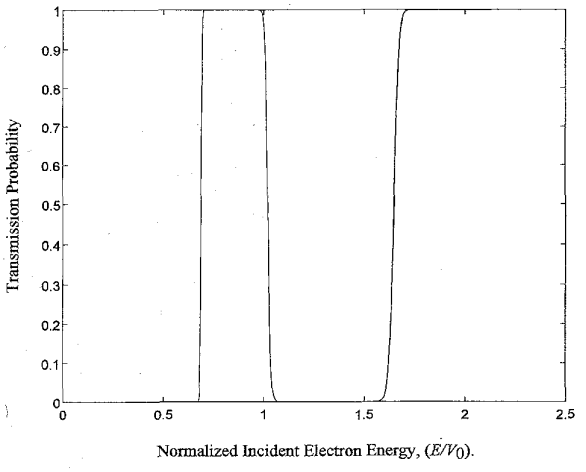

Fig. 2. Plot of the transmission probability as a function of normalized incident electron energy for an EBPF superlattice structure of 40 layer-pairs with $a = 32$ Å, $b = 32$ Å, $L = 2560$ Å, $\sigma_s = L/4$, and $V_0 = 0.45$ eV.

of potential is small compared with the electron wavelength, the reflection is expected to be small. By combining a slowly varying potential with a periodic superlattice which exhibits miniband structures, we thereby obtain an energy band-pass filter.

Consider one of the examples with the structure shown in Fig. 1. The superlattice is composed of 40 layer-pairs with a barrier width $a = 32$ Å and a well width $b = 32$ Å. Thus, the total length of the superlattice L is 2560 Å. The width σ_s of the modulating Gaussian function is taken to be $L/4$, and the barrier height V_0 is 0.45 eV. The electron effective mass is assumed to be 0.067 m_0 throughout the structure. In Fig. 2, the calculated transmission probability by the transfer-matrix method is plotted as a function of electron energy E. This figure shows nearly total transmission when the electron energy is in the range between 0.7–1.0 V_0 and above 1.7 V_0, while the transmission probability is zero when the electron energy lies outside these ranges. Flat passbands and stopbands result. The bands are flat and the boundaries between the passbands and stopbands are abrupt. This superlattice structure behaves like an energy band-pass filter (EBPF), which is similar to the frequency band-pass filter in circuit theory. This is quite different from the transmission characteristics of other types of superlattice structures. To make a comparison with regular superlattices, we calculate the transmission probability of a rectangular MQW (multiple

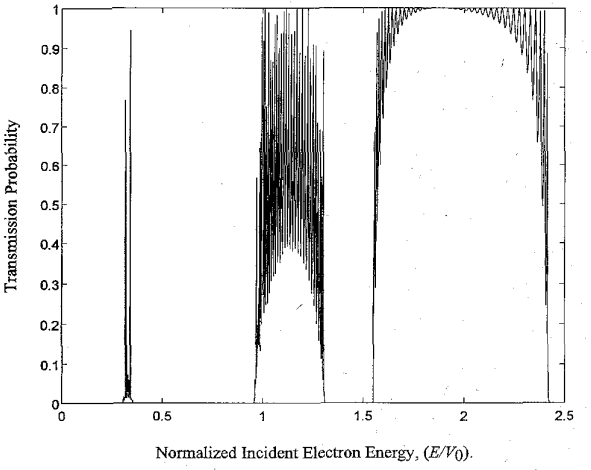

Fig. 3. Plot of the transmission probability as a function of normalized incident electron energy for a rectangular MQW structure of 40 layer-pairs, both barrier and well width are 40 Å, and the barrier height is 0.4 eV.

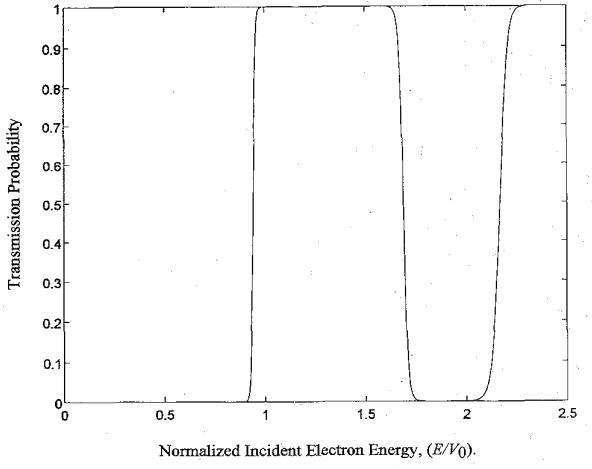

Fig. 4. Plot of the transmission probability as a function of normalized incident electron energy for an EBPF superlattice structure of 40 layer-pairs with $a = 32$ Å, $b = 32$ Å, $L = 2560$ Å, $\sigma_s = L/4$, and $V_0 = 0.3$ eV.

quantum wells) superlattice with 40 layer-pairs. The barrier height used here is 0.4 eV, the widths of both barriers and wells are 40 Å. Fig. 3 shows the calculated transmission probability versus energy. It indicates the existence of allowed minibands. But the transmission probability is not uniformly equal to one within each band. It is obvious that these conventional rectangular MQW superlattices do not have flat passbands as the EBPF does.

The position of the passbands and the widths of the bands can be easily adjusted by changing the layer parameters of the superlattice. Fig. 4 shows the calculated transmission probability for an EBPF with the same structure parameters as those used in Fig. 2 except V_0 is changed to 0.3 eV. We can see as the barrier height is reduced the position of the passband moves higher (relative to V_0) and the bandwidth becomes wider. Fig. 5 shows the calculated transmission probability of an EBPF with the same structure parameters as in Fig. 2 but with a shorter period of 50 Å ($a = b = 25$ Å). We again see that

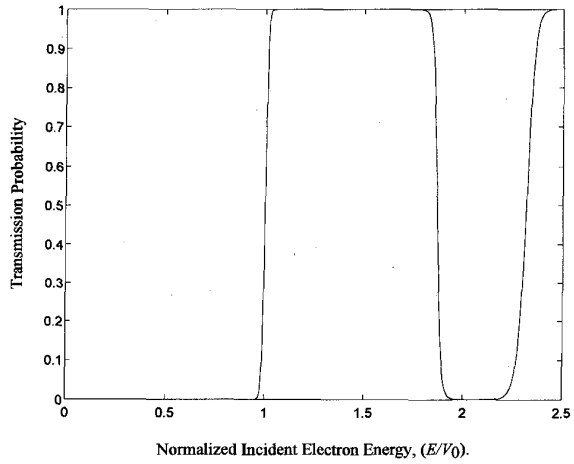

Fig. 5. Plot of the transmission probability as a function of normalized incident electron energy for an EBPF superlattice structure of 40 layer-pairs with $a = 25$ Å, $b = 25$ Å, $L = 2000$ Å, $\sigma_s = L/4$, and $V_0 = 0.45$ eV.

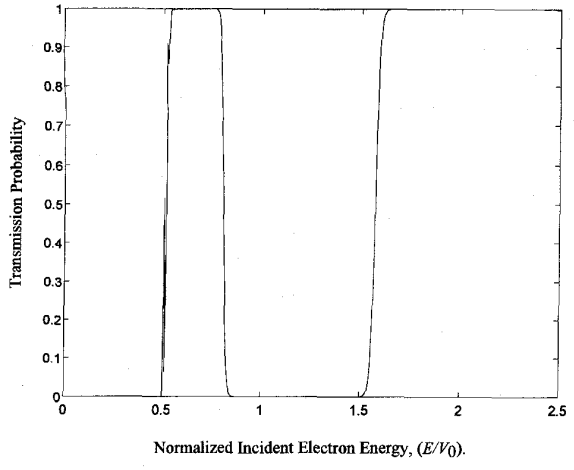

Fig. 6. Plot of the transmission probability as a function of normalized incident electron energy for an EBPF superlattice structure of 40 layer-pairs with $a = 28$ Å, $a + b = 64$ Å, $L = 2560$ Å, $\sigma_s = L/4$, and $V_0 = 0.45$ eV.

the energy of the passband moves higher and the bandwidth is wider. The trend is similar to that of a conventional superlattice where the quantized energy bands become higher and wider as the barriers and the wells of the superlattice become narrower. Fig. 6 shows the transmission probability spectrum of an EBPF with a smaller barrier width ($a = 28$ Å) but the period, $a + b$, and the rest of the parameters in Fig. 2 are kept unchanged. The position of the passband moves lower in this case. In summary, one can design an EBPF with desired bandwidth and band position by adjusting the parameters such as V_0, $a + b$, $a/(a + b)$, etc. The shape of the Gaussian function can be also changed. But in order for efficient modulation, the width (σ_s) of the Gaussian profile has to be much wider than the period of the superlattice. If we change σ_s to 1/16 of the total length (L) of the superlattice and leave other parameters the same as those in Fig. 2, the transmission spectrum becomes that shown in Fig. 7. Although the position of the passband remains about the same, the shape of the band profile becomes much poorer.

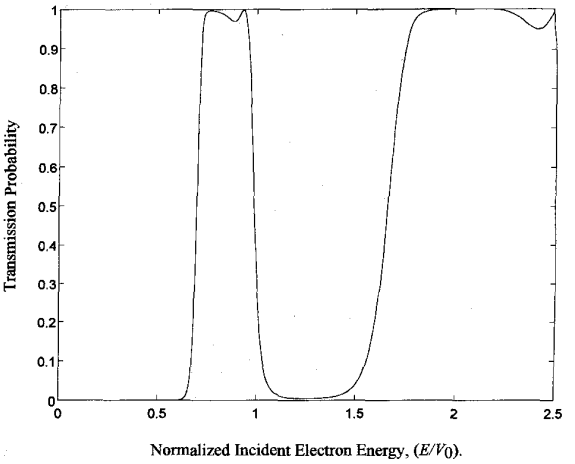

Fig. 7. Plot of the transmission probability as a function of normalized incident electron energy for an EBPF superlattice structure of 40 layer-pairs with $a = 32$ Å, $b = 32$ Å, $L = 2560$ Å, $\sigma_s = L/16$, and $V_0 = 0.45$ eV.

In this case, σ_s being only a little longer than the length of two periods of the superlattice, the incident electrons see a more abrupt change in potential profile, so a poorer transmission characteristic result.

From our numerical experience, we found that a gradually changing potential envelope function is crucial for a good energy band-pass filter, and a superlattice structure with a Gaussian potential profile does fulfill this requirement. An effective Gaussian envelope function can be also achieved by varying the widths of the barriers and the wells while keeping the period and the barrier height the same throughout the structure. We have performed calculation on such structure and similar band-pass transmission characteristics were obtained [11]. We have also tried other types of envelope functions, such as a triangular function, but none of them can work as well as the Gaussian function.

III. Time Evolution of Electron Wave Packet Through EBPF

To further check the concept discussed above, the time evolution of an electron wave packet propagating through an EBPF is calculated by numerically solving the Schrödinger equation. Our work follows closely that of Goldberg *et al.* [12] who first applied computer to demonstrate the motion of a Gaussian wave packet scattered from a square well or barrier. The time-dependent wave equation for a system governed by a time-independent potential $V(x)$ is:

$$-\frac{\hbar^2}{2m}\frac{\partial^2\psi}{\partial x^2} + V(x)\psi(x, t) = i\hbar\frac{\partial\psi}{\partial t}, \tag{1}$$

where $\psi(x, t)$ is the electron wave function, m is the effective mass of electron, and $\hbar$ is the Plank's constant. To solve this equation numerically, we first discretize the equation into a set of difference equations in a finite space-time grid. The wave function at each grid point is represented by

$$\psi_j^n = \psi(x_j, t_n),$$

where

$$j = 1, 2, 3, \cdots, J$$

and

$$n = 1, 2, 3, \cdots, N.$$

The difference equations are solved with the initial condition:

$$\psi(x, 0) = e^{ik_0 x} e^{-(x-x_0)^2/2\sigma_0^2}.$$

We see that this packet is centered at $x = x_0$ with a spread in x governed by σ_0. The factor $e^{ik_0 x}$ makes our initial wave function move to the right with an average momentum $\hbar k_0$, and k_0 is equal to $\sqrt{2mE}/\hbar$, where E is the average energy of the electron wave packet. We imagine that the physical system with which we work is situated in a large (one-dimensional) "box," and that the wave function for the system must vanish on the "walls" of the box. Thus, our boundary conditions may be stated in the form

$$\psi_0^n = \psi_j^n = 0, \quad \text{for all } n.$$

The criteria for a suitable choice of input parameters are given by Goldberg, *et al.* [12]. Fig. 8 shows the time series of a Gaussian wave packet impinging upon an EBPF which has the same structure as that used for Fig. 2. The average incident energy of the wave packet is chosen to be 0.425 V_0 and the spread of the packet, σ_0 is 400 Å, which corresponds to an energy uncertainty about 0.023 eV. From Fig. 2 we know that the energy of the wave packet lies within the stopband of the EBPF. Fig. 8 shows clearly that the wave packet is totally reflected. If the initial wave packet moves to the right with an incident energy $E = 0.85\ V_0$ and a same width of 400 Å (this corresponds to an energy uncertainty about 0.0325 eV), that is, when the incident energy lies in the passband of the EBPF, the time evolution of the wavepacket, shown in Fig. 9, is totally different. Complete transmission happens and no noticeable reflection is detected. Although the scattering strength is strong when the wave packet is moving within the superlattice, there is no distortion for the transmitted wave except the spreading of the wave packet. To make a comparison between EBPF and the conventional rectangular MQW, we also simulated the scattering of a Gaussian wave packet by a rectangular MQW with the transmission characteristics shown in Fig. 3. The wavepacket has an incident energy of 1.15 V_0 with a width of 0.036 eV (the energy spreading again corresponds to a spatial width of 400 Å) which lies within the miniband of the MQW. The time evolution of the wave packet moving through such a structure is shown in Fig. 10. As expected, partial reflection and partial transmission are observed even the energy of the wave packet is within the miniband of the MQW. From the numerical results presented here, it is clear that EBPF's can really serve as energy band-pass filters for electrons.

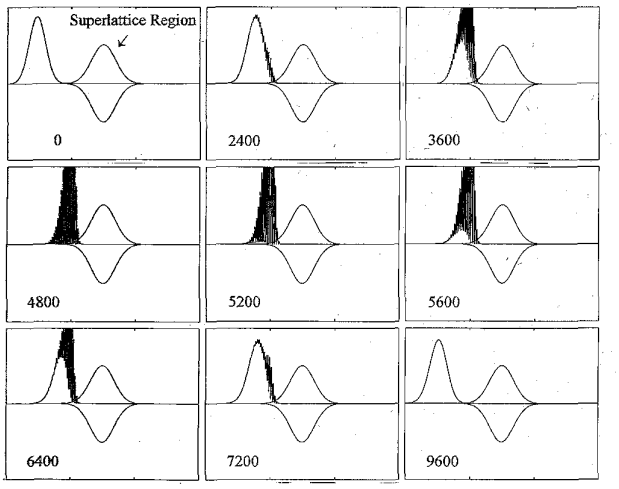

Fig. 8. Gaussian wave-packet scattering from an EBPF superlattice structure with the same structure parameters in Fig. 2. The average incident energy is 0.425 V_0. Numbers denote the time of each configuration in arbitrary units. The region enclosed by the positive and negative Gaussian function is the superlattices as shown in Fig. 1.

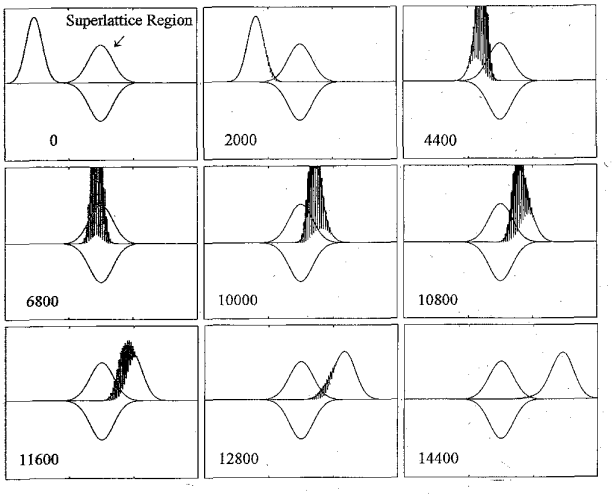

Fig. 9. Gaussian wave-packet scattering from an EBPF superlattice structure with the same structure parameters in Fig. 2. The average incident energy is 0.85 V_0. Numbers denote the time of each configuration in arbitrary units. The region enclosed by the positive and negative Gaussian function is the superlattices as shown in Fig. 1.

IV. Quantum-Mechanical Wave Impedance Matching

The generalized concept of quantum-mechanical wave impedance (QMWI) was first introduced by Khondker *et al.* [13]. This concept is analogous to the impedance in the well-developed transmission line theory. The quantum-mechanical transmission probability can be easily calculated using this method. The QMWI at any plane x can be defined as

$$Z(x) = \frac{2\hbar\psi'(x)}{jm\psi(x)}, \tag{2}$$

where $Z(x)$ is the wave impedance looking into the positive x direction, $j = \sqrt{-1}$, m is the electron effective mass, $\psi(x)$ and $\psi'(x)$ are the electron wave function and its spatial derivative, respectively, for the potential problem interested. For an arbitrary-shaped potential we can approximate the potential

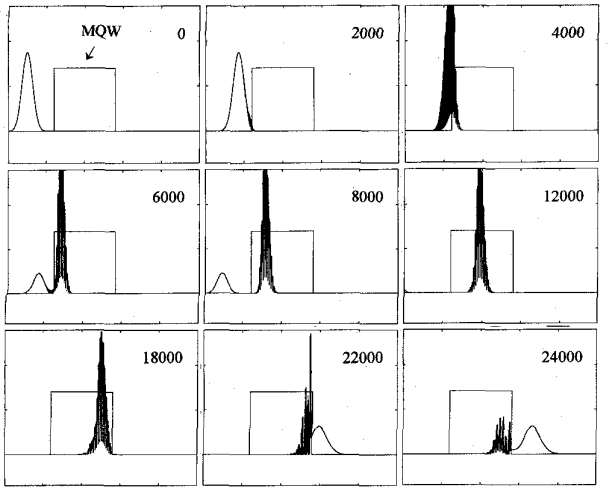

Fig. 10. Gaussian wave-packet scattering from a rectangular MQW with the same structure parameters in Fig. 3. The average incident energy is 1.15 V_0, where V_0 is the barrier height of MQW. Numbers denote the time of each configuration in arbitrary units. The region enclosed by rectangle is the MQW structure.

by multistep functions with a sequence of N segments. Thus, if x_i and x_{i+1} are the boundaries of segment i, the QMWI at x_i can be calculated by

$$Z(x_i) = Z_{0i}\frac{Z(x_{i+1})\cosh(\gamma_i l_i) - Z_{0i}\sinh(\gamma_i l_i)}{Z_{0i}\cosh(\gamma_i l_i) - Z(x_{i+1})\sinh(\gamma_i l_i)}, \quad (3)$$

where

$$\gamma_i = j\sqrt{\left(\frac{2m}{\hbar^2}\right)(E - V_i)}, \quad (4)$$

$$l_i = x_{i+1} - x_i,$$

and

$$Z_{0i} = \frac{2\gamma_i \hbar}{jm} \quad (5)$$

is the characteristic impedance of the medium. Equation (3) expresses the QMWI at x_i in terms of the QMWI at x_{i+1}, and γ_i, l_i, and Z_{0i}. Once $Z(x_i)$ is calculated, we can repeat the process for segment $i-1$ to calculate $Z(x_{i-1})$ using γ_{i-1}, l_{i-1}, and Z_{0i-1}. Repeatedly using (3)–(5), we can evaluate the total input impedance of EBPF and treat the whole superlattice structure as an equivalent load impedance Z_{EBPF}. Thus, the reflection coefficient $\rho(E)$ for the wave amplitude can be calculated as

$$\rho(E) = \frac{Z_{\mathrm{EBPF}} - Z_0}{Z_{\mathrm{EBPF}} + Z_0}, \quad (6)$$

where Z_0 is the characteristic QMWI of the bulk semiconductor outside the EBPF, and the transmission probability is given by

$$T(E) = 1 - |\rho(E)|^2. \quad (7)$$

We have used (7) to calculate the transmission probability for an EBPF with the identical structure parameters used in Fig. 2. The result is the same as that calculated by the transfer-matrix method shown in Fig. 2.

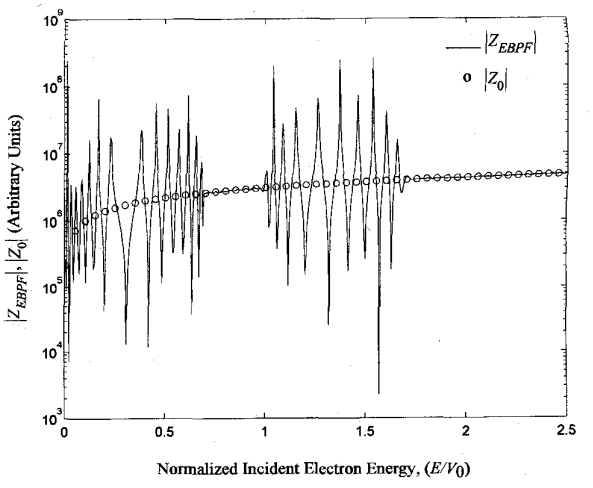

Fig. 11. The absolute values of quantum-mechanical wave impedance (QMWI) Z_{EBPF} and Z_0 as a function of normalized incident electron energy with the same structure parameters in Fig. 2.

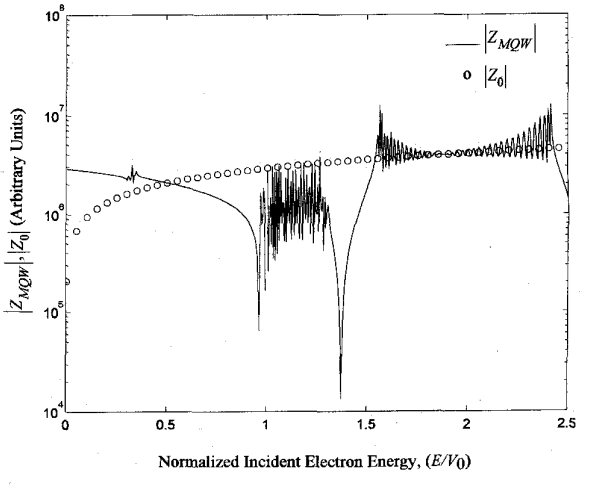

Fig. 12. The absolute values of quantum-mechanical wave impedance (QMWI) Z_{MQW} and Z_0 as a function of normalized incident electron energy with the same structure parameters in Fig. 3.

From the transmission line theory [14] we know that matched condition occurs when the load impedance is equal to the characteristic impedance of the transmission line. Under such condition, the reflection coefficient $\rho(E)$ in (6) should be zero and the transmission probability $T(E)$ in (7) should be equal to 1. Fig. 11 shows the QMWI, Z_{EBPF}, and Z_0 as functions of energy of an EBPF with the same structure parameters used in Fig. 2. It clearly demonstrates that when the incident energy lies in the passband, Z_{EBPF} matches Z_0 completely, while outside the passband, large impedance mismatch exists. The result is in good agreement with that calculated in Fig. 2. Fig. 12 shows the calculated QMWI, Z_{MQW}, and Z_0 as functions energy for a rectangular MQW, which has the structure parameters the same as those used in Fig. 3. The figure demonstrates that impedance mismatch exists everywhere, even in the minibands. This explained why a rectangular MQW structure does not have the property of total transmission for a Gaussian wave packet.

V. Conclusion

An energy band-pass filter (EBPF) using superlattice structures with a Gaussian envelope profile is proposed. Adjustable flat transmission bands and reflection bands are obtained by properly choosing the layer parameters. When an electron impinges upon an EBPF, it will be completely reflected or transmitted depending on whether the incident energy lies in the stopband or passband of the EBPF. Simulations of the time evolution of wave packets traveling through such structures clearly demonstrate the bandpassing characteristics of EBPF's. The phenomenon of total transmission can be successfully explained by using the concept of wave impedance analogous to that in the transmission line theory.

References

[1] L. Esaki and R. Tsu, "Superlattice and negative differential conductivity in semiconductors," *IBM J. Res. Dev.,* vol. 14, pp. 61–65, 1970.

[2] H. L. Stormer, J. P. Eisenstein, A. C. Gossard, W. Wiegmann, and K. Baldwin, "Quantization of the Hall effect in an anisotropic three-dimensional electronic system," *Phys. Rev. Lett.,* vol. 56, pp. 85–88, 1986.

[3] J. Depeyrot, P. Tronc, G. Wang, and J. F. Palmier, "Enhancement of the −1 staker ladder transition in a superlattice: A proposal for a new electro-optical modulator with a high extinction ratio," *Superlattices and Microstructures,* vol. 15, pp. 297–301, 1994.

[4] T. H. Wood, "Multiple quantum well (MQW) waveguide modulators," *J. Lightwave Technol.,* vol. 6, pp. 743–757, 1988.

[5] G. I. Stegeman, E. M. Wright, N. Finlayson, R. Zanoni, and C. T. Seaton, "Third order nonlinear integrated optics," *J. Lightwave Technol.,* vol. 6, pp. 953–970, 1988.

[6] K. Iga, H. Uehara, and F. Koyama, "Electron reflectance of multiple quantum barrier (MQB)," *Electron. Lett.,* vol. 22, pp. 1008–1010, 1986.

[7] F. Capasso, K. Mohammed, and A. Y. Cho, "Resonant tunneling through double barriers, perpendicular quantum transport phenomena in superlattices, and their device applications," *IEEE J. Quantum Electron.,* vol. QE-22, pp. 1853–1869, 1986.

[8] T. Nakagawa, N. Kawai, K. Ohta, and M. Kawashima, "Time evolution of electron wave-packets in modulated superlattices and at their boundaries," *Superlattices and Microstructures,* vol. 1, pp. 217–221, 1983.

[9] D. Mukherji and B. R. Nag, "Band structure of semiconductor superlattices," *Phys. Rev.,* vol. B-12, pp. 4338–4345, 1975.

[10] M. Lundstrom, *Fundamental of Carrier Transport.* Reading, MA: Addison-Wesley, 1990, pp. 10–11.

[11] H. H. Tung and C. P. Lee, "A quantum-mechanical bandpass filter using semiconductor superlattices," to be published.

[12] A. Goldberg. H. M. Schey, and J. L. Schwartz, "Computer-generated motion pictures of one-dimensional quantum-mechanical transmission and reflection phenomena," *Amer. J. Phys.,* vol. 35, pp. 177–186, 1967.

[13] A. N. Khondker, M. R. Khan, and A. F. M. Anwar, "Transmission line analogy of resonance tunneling phenomena: The generalized impedance concept," *J. Appl. Phys.,* vol. 63, pp. 5191–5193, 1988.

[14] D. K. Cheng, *Field and Wave Electromagnetics.* Reading, MA: Addison-Wesley, 1983, pp. 390–395.

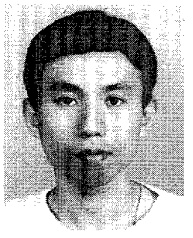

Hsin-Han Tung was born in Chia-Yi, Taiwan, in 1964. He received the B.S. and M.S. degrees in electrical engineering from the National Chun-Shen University in 1986 and 1988, respectively.

Currently, he is working toward the Ph.D. degree in electronic engineering at the National Chiao Tung University, Taiwan, ROC. His research interests include quantum tunneling effects in semiconductor superlattices, wave propagation in layered medium, and electron wave devices. He is also a Lecturer at the National Lien-Ho Junior College of Technology since 1990.

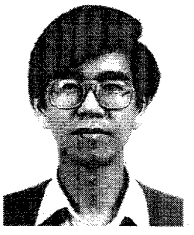

Chien-Ping Lee (M'80–SM'94) received the B.S. degree in physics from National Taiwan University in 1971 and the Ph.D. degree in applied physics from the California Institute of Technology, Pasadena, in 1978.

While at Caltech, he worked on GaAs-based integrated optics. He was credited with the design and fabrication of several important optoelectronic components, including the first integrated optoelectronic circuit, which consists of a laser and a Gunn device fabricated on a same substrate. After graduation, he joined Bell Laboratories, where he worked on integrated optics and semiconductor lasers. He joined Rockwell International in 1979 and worked on GaAs integrated circuits. He did extensive work on substrate related effects such as the orientation effect and the backgating effect. Later, he became the Manager of the Heterostructure FET's Department in charge of the development of HEMT integrated circuits. In 1987, he joined National Chiao Tung University in Taiwan to be a Professor and the Director of the Semiconductor Research Center. He was also the first Director of the National Nano Device Laboratory. In 1990, he returned to Rockwell and was Manager of the Advanced Device Laboratory. In 1990, he went back to Rockwell and was Manager of the Advanced Device Concept Department. He returned to Taiwan in 1992 and is currently a Professor in the Institute of Electronics of National Chiao Tung University. His research interests are in the areas of III–V optoelectronic devices, MBE technology, GaAs IC's, heterostructure devices and physics, and device simulation.

Dr. Lee received the Engineer of the Year award in 1982 for his contribution in GaAs IC and HEMT technologies. He received the best teacher award from the Ministry of Education in 1993 and the outstanding research award from the National Science Council in 1994.